solution, which is identical with the monodisperse theory (the general linear viscoelastic theory), as MW is normalized with respect to $M_e'$ given by eq 1.[8]

On the other hand, as a binary blend becomes monodisperse in three ways, the $G(t)$ functional form transforms into the monodisperse theory (for a melt). For $M_H \rightarrow M_L$ or $M_L \rightarrow M_H$, a transition of $\mu_T(t/\tau_T)$ from being time dependent to being time independent is indicated. This transition corresponds to the conclusion that the tube renewal process is negligible in a monodisperse system and the regional constraint release process is effective in a binary blend.

In a previous report,[8] based on the tube sizes in monodisperse melts and concentrated solutions, we have proposed the tube size enlargement effect, which mainly occurs in the terminal region associated with the high MW component in a binary blend. Here, the experimental results of binary blends in the terminal region of the high MW component are compared with the calculated $G(t)$ curves by using different $M_e''$ values and the measured spectra of the pure monodisperse melts of the high MW components. The comparison allows us to quantify the tube size enlargement effect. The $\tau_C'/\tau_C$ and $M_e'/M_e$ values obtained from extrapolating the obtained $\tau_C''/\tau_C$ and $M_e''/M_e$ values as $M_L$ becomes zero are in good agreement with the theoretical values. These results join the previous studies supporting the validity of the general linear viscoelastic theory as applied to monodisperse melts and concentrated solutions and justifies the phenomenological description of the tube size enlargement effect occurring in binary blends.

The proposed $G(t)$ functional form (the blending law) greatly advances our understanding of the polymer dynamics in binary blends. This will be further demonstrated in the line-shape analyses of the linear viscoelastic spectra of binary blends as reported in the accompanying paper.

## References and Notes


(1) Doi, M.; Edwards, S. F. *J. Chem. Soc., Faraday Trans. 2* **1978**, *74*, 1789.
(2) Doi, M.; Edwards, S. F. *J. Chem. Soc., Faraday Trans. 2* **1978**, *74*, 1802.
(3) Doi, M.; Edwards, S. F. *J. Chem. Soc., Faraday Trans. 2* **1978**, *74*, 1818.
(4) Doi, M.; Edwards, S. F. *J. Chem. Soc., Faraday Trans. 2* **1979**, *75*, 38.
(5) Lin, Y.-H. *Macromolecules* **1984**, *17*, 2846.
(6) Lin, Y.-H. *Macromolecules* **1986**, *19*, 159.
(7) Lin, Y.-H. *Macromolecules* **1986**, *19*, 168.
(8) Lin, Y.-H. *Macromolecules* **1987**, *20*, 885.
(9) Lin, Y.-H. *Macromolecules* **1985**, *18*, 2779.
(10) Lin, Y.-H. *Macromolecules* **1987**, *20*, 3080.
(11) Lin, Y.-H., see ref. 52 of the paper by Struglinski and Graessley (ref 16).
(12) See ref 21 of ref 6.
(13) Rouse, P. E., Jr. *J. Chem. Phys.* **1953**, *21*, 1271.
(14) Doi, M.; Graessley, W. W.; Helfand, E.; Pearson, D. S. *Macromolecules* **1987**, *20*, 1900.
(15) Mooney, M. *J. Polym. Sci.* **1959**, *34*, 599.
(16) Struglinski, M. J.; Graessley, W. W. *Macromolecules* **1985**, *18*, 2630.
(17) Pearson, D. S. *Rubber Chem. Technol.* **1987**, *60*, 439.
(18) Graessley, W. W. *Adv. Polym. Sci.* **1982**, *47*, 67.
(19) Klein, J. *Polym. Prepr. (Am. Chem. Soc., Div. Polym. Chem.)* **1981**, *22*, 105.
(20) Klein, J. *Macromolecules* **1986**, *19*, 105.
(21) Daoud, M.; de Gennes, P.-G. *J. Polym. Sci., Polym. Phys. Ed.* **1979**, *17*, 1971.
(22) Watanabe, H.; Sakamoto, T.; Kotaka, T. *Macromolecules* **1985**, *18*, 1008.


# Line-Shape Analyses of the Linear Viscoelastic Spectra of Binary Blends in Terms of the Proposed $G(t)$ Functional Form. 2


**Y.-H. Lin**

*Exxon Chemical Company, Baytown Polymers Center, Baytown, Texas 77522.*


*Received September 16, 1988; Revised Manuscript Received January 20, 1989*



ABSTRACT: The linear viscoelastic spectra of a series of binary blends consisting of nearly monodisperse polymers have been measured and analyzed in terms of the proposed binary theory. The unique features of the line shapes of the spectra are quantitatively described by the proposed theory in a consistent manner. Very significantly, it is shown that the reptation time of the low molecular weight (MW) component in a binary blend is identical with that in its pure melt state. This is in agreement with the expectation from the conclusion that the tube renewal process is negligible in a monodisperse polymer. The characteristic time associated with the regional constraint release process, $\mu_T(t/\tau_T)$, is about seven times larger than the reptation time of the low MW component regardless of the MWs and weight fractions of the components. This indicates that the $\mu_T(t/\tau_T)$ process should not be described by the "Rouse tube" motion. In the terminal region of the high MW component, the tube size enlargement effect is included in the line-shape analyses by using an effective entanglement MW ($M_e''$). The extrapolated values of $M_e''$ to the concentrated solution cases ($M_L \rightarrow 0$) are in good agreement with the theoretical values ($M_e' = M_e W_H^{-1}$).


## I. Introduction

A functional form for the stress relaxation moduli $G(t)$ of blends consisting of two (nearly) monodisperse polymers has been proposed[1] (referred to as the binary theory below). This functional form is built upon the monodisperse theory,[2] which has been extensively and quantitatively tested with experimental results.[3-8] Along with the proposition of the binary theory, specifically we have pointed out the following three effects, which were described in paper 1:[1] the relative fast reptation motion of the low molecular weight (MW) component causes the regional constraint release process on the high MW chain tube; tube size enlargement occurs (mainly) in the terminal region associated with the high MW component; transition of $\mu_T(t/\tau_T)$ from being time dependent to being time independent takes place as $M_H \rightarrow M_L$ or $M_L \rightarrow M_H$.

Polymer dynamics in a binary blend are much more complicated than those in a monodisperse system. In a

0024-9297/89/2222-3080$01.50/0 

monodisperse system, the bulk linear viscoelastic behavior is reduced to that of a single averaged polymer chain, for the tube renewal process is negligible.[2-8] In a binary blend, the regional constraint release effect on the long-chain tube caused by the relatively fast reptation motion of the short chains needs to be considered; the system is becoming a many-body problem.

Because of the greater complexity in binary blends, we have to describe the first two effects listed above phenomenologically and include such phenomenological descriptions to analyze the line shapes of the linear viscoelastic spectra. The line-shape analyses of the binary blends are basically not affected by the shortcoming of having to involve the phenomenological descriptions. In fact, the features of the line shapes are uniquely described by the proposed functional form in a consistent manner. Furthermore, we were able to obtain the systematic change of the $\tau_C''/\tau_C$ ratio with $M_L$ as reported in the accompanying paper and the $S$ parameter (see eq 2) as a constant (independent of MWs and weight fractions of both the high and low MW components) from the line-shape analyses reported below. The successful results of the line-shape analyses not only justify the involved phenomenological descriptions of the effects but also shed light on the important polymer dynamic modes in binary blends.

Very significantly, it is shown that the reptation time of the low MW component in a binary blend is identical with that in its pure melt state. This is in agreement with the expectation from the conclusion, which we have reached,[1-8] that the tube renewal process is negligible in a monodisperse polymer.

The results that $\mu_T(t)$ is best described by a box-type relaxation function and that $S$ is a constant lead us not to take the view that the $\mu_T(t)$ process can be described by the "Rouse tube" motions, as recently suggested by Struglinski and Graessley,[9] Doi et al.,[10] and Pearson,[11] who have adopted the basic picture of the proposed binary theory. As early as 1983, we found that $S$ should be a constant in our preliminary experimental results.[12] Here, we report the results of refined measurements confirming our early notion.

## II. Theory

Here we are concerned with the line shapes of the linear viscoelastic spectra of the binary blends in the a region and a small part of the b regions (see Figure 1 of the accompanying paper). For testing the proposed $G(t)$ functional form with experimental results, we can at best use *nearly* monodisperse samples as the components in the binary blends. Closely related to the transition of the $\mu_T(t/\tau_T)$ process from being time dependent to being time independent as $M_L \rightarrow M_H$ or $M_H \rightarrow M_L$, two ranges of molecular weight distribution (MWD) need be considered separately in such binary blends: (a) the very narrow MWD in a nearly monodisperse component, where the linear additivity law of the contributions from the subcomponents is applicable because the tube renewal process is negligible in a nearly monodisperse system; (b) the far range MWD that is determined by the MW values ($M_H$ and $M_L$) and the weight fraction ($W_H$ and $W_L$) of the two nearly monodisperse components.

The regional constraint release process that occurs in case b is a main subject of interest in this study.

To avoid the confusion that may arise between these two ranges of MWD, in the following equation for $G(t)$ we spell out the contributions from all MW components and subcomponents:

$$G(t) = G_N[1 + \mu_A(t/\tau_A)]\{W_L\{\sum_i W_i^L[1 + \tfrac{1}{4}\mu_X(t/\tau_{Xi}^L)] \times [B_i^L\mu_B(t/\tau_{Bi}^L) + C_i^L\mu_C(t/\tau_{Ci}^L)]\} + W_H[W_L\mu_T(t/\tau_T) + W_H]\{\sum_j W_j^H[1 + \tfrac{1}{4}\mu_X(t/\tau_{Xj}^H)][B_j^H\mu_B(t/\tau_{Bj}^H) + C_j^H\mu_C(t/\tau_{Cj}^H)]\}\} \quad (1)$$

where $w_i^L$ and $w_j^H$ denote respectively the weight fraction of the $i$th subcomponent in the nearly monodisperse low MW component of weight fraction $W_L$ and the weight fraction of the $j$th subcomponent in the nearly monodisperse high MW component of weight fraction $W_H$. The regional constraint release process on the high MW chain tube, $\mu_T(t/\tau_T)$, is assumed to have a single exponential decay form for a phenomenological description (see the Appendix)

$$\mu_T(t/\tau_T) = \exp(-t/\tau_T) = \exp(-t/S\tau_C^L) \quad (2)$$

and its relaxation time $\tau_T$ is proportional to the *single* reptation time ($\tau_C^L$) of the low MW component at its weight-average MW. This simplification makes our computer calculation easier and for our purpose does not sacrifice the quality of the line-shape analyses of the linear viscoelastic spectra as shown below.

## III. Experiment and Computer Calculation

It is relatively easy to calculate the linear viscoelastic spectra in the time domain from eq 1. This influenced us in the early stage of this study to measure the linear viscoelastic spectra in the time domain for comparison with the theory. Because of the wide dynamic range of the $G(t)$ spectrum of a blend sample and the fact that measurements at several different temperatures are required to make a master curve, data accuracy is demanded of each spectrum, which is only met by the measurements in the time domain in favorable situations.

Being not totally satisfied with our $G(t)$ data, we switched to measurements in the frequency domain, where, because of the process of correlating strain and stress signals with a standard sine wave to calculate the in-phase ($G'(\omega)$) and out-of-phase ($G''(\omega)$) components, the data accuracy is greatly improved. Calculating the $G'(\omega)$ and $G''(\omega)$ spectra numerically from the $G(t)$ spectra, which have been calculated from eq 1, is difficult to do, because too many decades are involved. It is possible to write the Fourier transform of eq 1 in a computer program, although it is extremely lengthly. In so doing, besides the simplification of the relaxation form for $\mu_T(t/\tau_T)$ described above, we have also simplified the $\mu_X(t/\tau_X)$ process to involve only one term corresponding to the weight-average MW of each component. This simplification should be quite all right because the MW dependence of $\tau_X$ is relatively weak ($\tau_X \propto M_e M$) compared to $\tau_B$ and $\tau_C$. The summation terms up to $P = 9$ for the $\mu_A(t)$ process and up to $P = 35$ for the $\mu_B(t)$ and $\mu_C(t)$ processes are included in the calculation of the $G'(\omega)$ and $G''(\omega)$ spectra (see paper 1). This is more than enough for the accuracy involved.

The nearly monodisperse polystyrene samples F80 ($M_w$ = 775 000), F35 ($M_w$ = 355 000), F10 ($M_w$ = 100 000), and F4 ($M_w$ = 44 900) used to make the binary blend samples for the present study have been described in previous papers.[3,6] Binary blends for linear viscoelastic spectrum measurements have been prepared at the following percentage ratios: F35/F10 = 75/25, 50/50, 25/75; F35/F4 = 75/25, 50/50, 25/75; F80/F10 = 50/50, 25/75; and F80/F4 = 50/50, 25/75. The details of the linear viscoelastic spectrum measurements and of the preparation of the samples are as described before.[2-4]

## IV. Comparison of the Measured and Calculated Spectra

The $G(t)$ functional form (eq 1) for a binary blend involves several parameters. Most parameters are predetermined for calculating the linear viscoelastic spectra. $W_L$ and $W_H$ are determined in the sample preparation. The MWDs ($w_i^L$ or $w_j^H$) of the components (F80, F35, F10, and F4) used in the present calculations are identical with those which have been obtained in the linear viscoelastic spectrum line-shape analyses of the nearly monodisperse samples in pure melt in terms of the monodisperse theory.[2,3] This is in accord with the relations between the monodisperse theory and the binary theory as described in paper 1.[1] MWDs consisting of three (sub)components for F80 and F35 (e.g., see Figure 7 of ref 2 for the MWD of F80) have been obtained through nonlinear least-squares fitting to the linear viscoelastic spectra of the nearly monodisperse samples. See ref 2 for the details of the computer fitting procedure. The high MW samples (F80 and F35) normally have a broader MWD and contain some low MW tail (see Figure 16 of ref 2 and the Appendix of ref 3). The low MW components of such a sample cause a steeper decline in the plateau region and reduce the sharpness of the "corner" in the terminal region. This in effect broadens the MWD that can be extracted from the line shape of the linear viscoelastic spectrum.[3] The obtained MWDs ($M_w/M_n$ = 1.24 for F80 and $M_w/M_n$ = 1.13 for F35) are, thus, somewhat greater than the GPC values. Also, because of this MWD effect, the $K$ constants (equivalent to the frction constant, see eq 6 of paper 1) obtained from the line-shape analyses for F80 and F35 (denoted as $K_H$) are about 20–30% smaller than those (denoted as $K_L$) at lower MWs: F10 and F4[2,3,6] (see ref 3 for the explanation). The MWDs for F10 and F4 are the Schulz MWD shown in Figure 16 of ref 3.

We have also observed that in the high MW region, the $K$ constant in the $\mu_A(t)$ process (denoted as $K'$) is about 3.3 times (after an ~30% correction of an effect due to MWD) larger than the $K$ value in the $\mu_B(t)$ and $\mu_C(t)$ processes. At around $M/M_e$ = 10, $K'/K$ begins to decline with decreasing MW and reaches a limiting value of 1 at $M/M_e \sim 1$. These observed phenomena have been well explained as due to the extra free volume associated with the polymer chain ends,[2-4] which is closely related to the topological constraint of chain entanglement. In the present line-shape analyses for the binary blend samples, the $K'/K$ ratio is an adjustable parameter. ($K$ is the average of $K_H$ and $K_L$; it is shown below that the obtained $K_H$ and $K_L$ values differ no more than 30%.)

The remaining parameters are the $S$ constant in the $\mu_T(t/\tau_T)$ process and the effective $M_e$ value (denoted as $M_e''$), to account for the tube size enlargement effect clearly observed in the terminal region of the high MW component, which has been described in paper 1.[1] We have found that $S$ is constant (~7) for all the studied binary blend samples. Except for the F80/F10 = 25/75, F80/F4 = 25/75, F35/F4 = 25/75, and F35/F10 = 25/75 blends (whose $M_e''$ values will be described later), the $M_e''$ values used are calculated from the following equation for the shifting factor $\tau_C''/\tau_C$:

$$\tau_C''/\tau_C = M_e[1 - (M_e''/M)^{0.5}]^2/M_e''[1 - (M_e/M)^{0.5}]^2 \quad (3)$$

which is obtained from eq 14 of paper 1.[1] The shifting factors have been obtained from superposing the spectrum of each binary blend sample onto that of a pure melt of the high MW component (F80 or F35) in the terminal region as described in paper 1. Listed in Table I are the parameters used in the calculations of the linear viscoelastic spectra for the studied blend samples. The comparisons of the calculated and measured linear viscoelastic spectra for F35/F4 = 75/25, 50/50, 25/75; F35/F10 = 75/25, 50/50, 25/75; F80/F4 = 50/50, 25/75; and F80/F10 = 50/50, 25/75 are shown in Figures 1–10, respectively. (See below for the choice of the $M_e''$ value for the samples

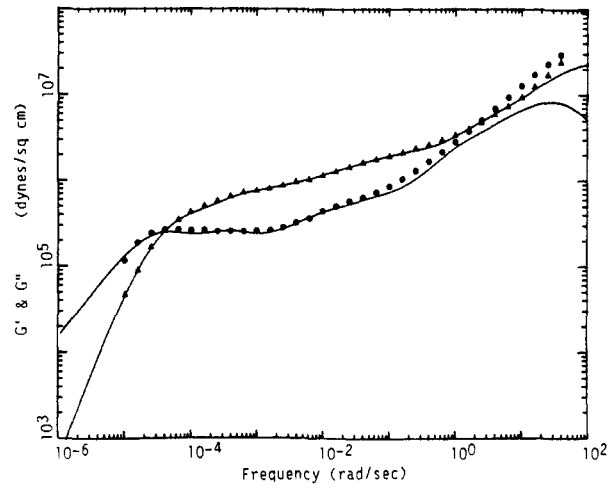


**Figure 1.** Comparison of the measured and calculated linear viscoelastic specctra of the F35/F4 = 75/25 blend [(▲) the storage modulus $G'$ and (●) the loss modulus $G''$]. See Table I for the values of the parameters used in the calculation.

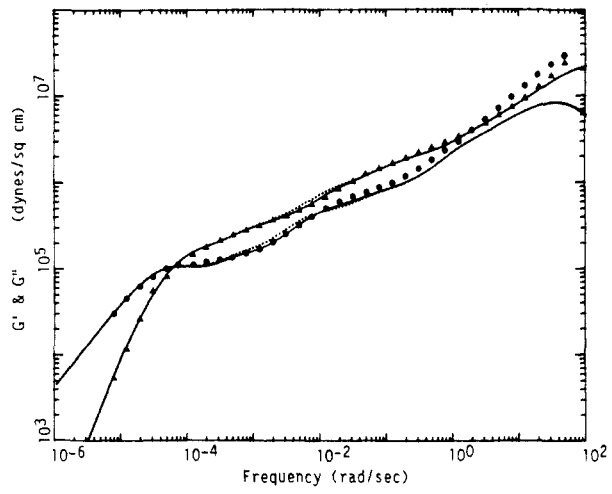


**Figure 2.** Same as Figure 1 for the F35/F4 = 50/50 blend. Also shown is the spectra calculated with $S$ = 10 (···) for comparison with the spectra (—) calculated with $S$ = 7.

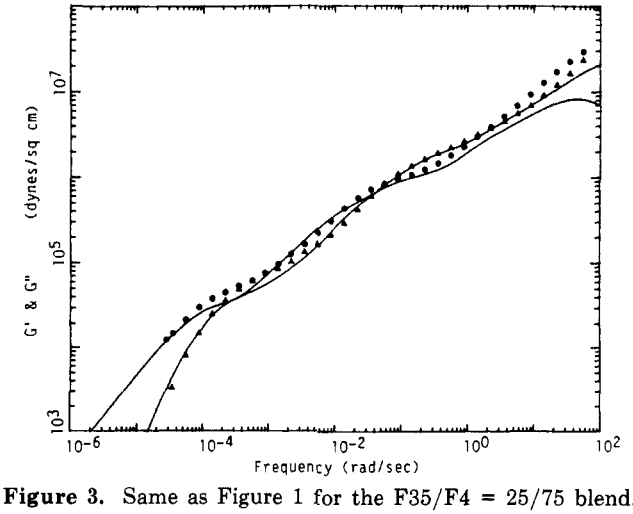


**Figure 3.** Same as Figure 1 for the F35/F4 = 25/75 blend.

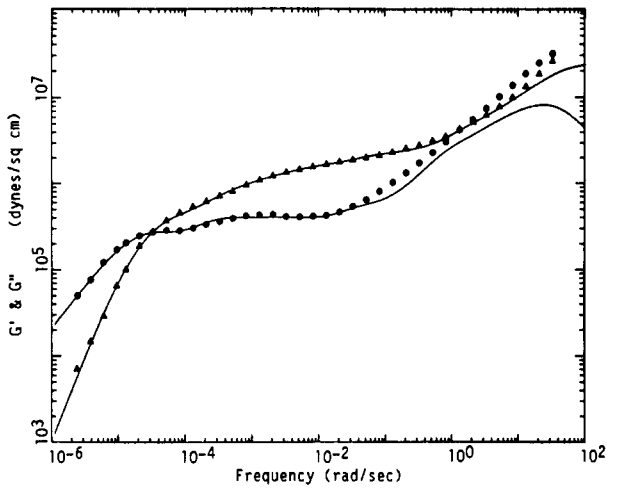


**Figure 4.** Same as Figure 1 for the F35/F10 = 75/25 blend.

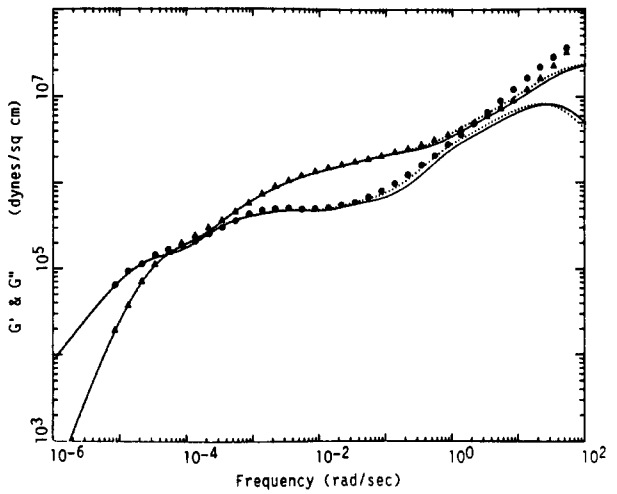


**Figure 5.** Same as Figure 1 for the F35/F10 = 50/50 blend. Also shown in the spectra (···) calculated with $K'/K = 3.36$ for comparison with the spectra (—) calculated with $K'/K = 2.8$.

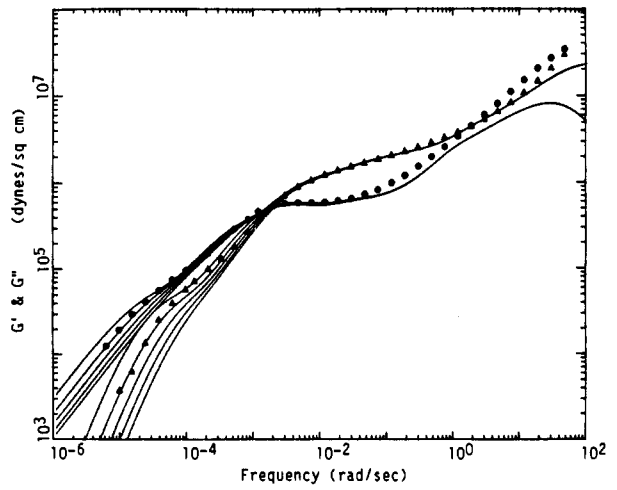


**Figure 6.** Same as Figure 1 for the F35/F10 = 25/75 blend. Shown are the theoretical curves calculated with $M_e''/M_e = 1$, 1.5, 2, 2.5, and 3 (from left to right) while keeping the other parameters the same (see Table I). The theoretical curve of $M_e''/M_e = 1.5$ has the best agreement with the experiment results.

of F80/Y or F35/Y = 25/75.)

The theoretical curves describe the unique features associated with individual measured spectra very well. Particularly noteworthy are the predictions of the triple crossovers between $G'(\omega)$ and $G''(\omega)$ (not including the crossover in the high-frequency region) of the spectra of

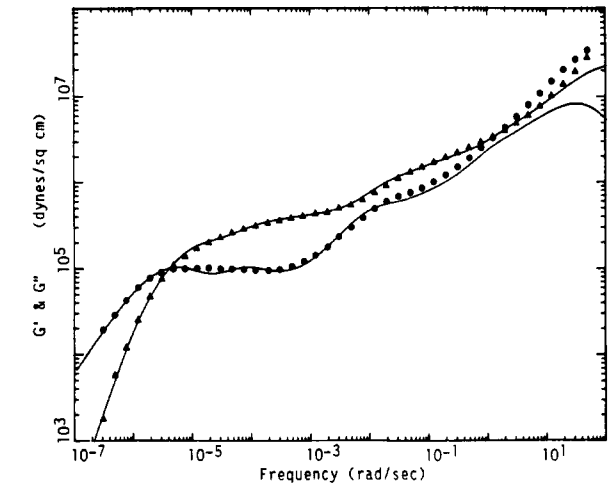


**Figure 7.** Same as Figure 1 for the F80/F4 = 50/50 blend.

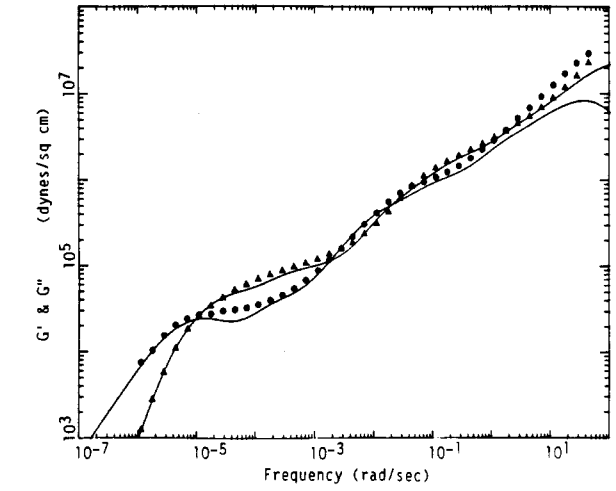


**Figure 8.** Same as Figure 1 for the F80/F4 = 25/75 blend.

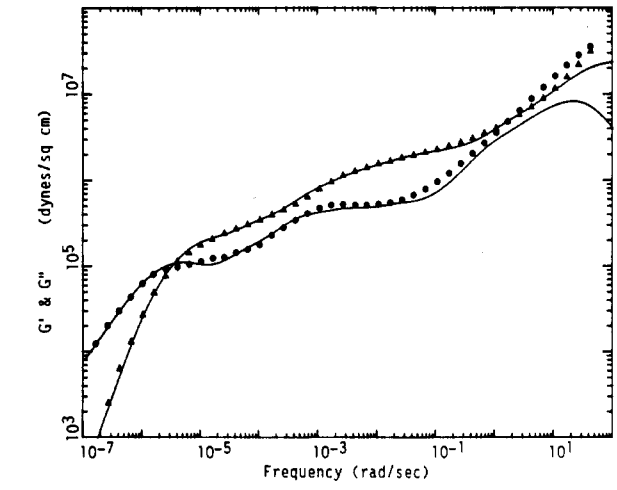


**Figure 9.** Same as Figure 1 for the F80/F10 = 50/50 blend.

F80/F4 = 25/75 (Figure 8) and F80/F10 = 25/75 (Figure 10). In the high-frequency region, the differences between the calculated and measured $G'(\omega)$ and $G''(\omega)$ results are due to the glassy relaxation process, which is not included in the theory. As explained before,[3,6] in the case of $G'(\omega)$, the effect of the glassy relaxation process is localized in the frequency region where it occurs; in the case of $G''(\omega)$, the effect is extended to the lower frequency region. For this reason, the theory does not account for the crossover between $G'(\omega)$ and $G''(\omega)$ in the high-frequency region. The same occurs in the line-shape analyses for nearly monodisperse melts[3,4] and concentrated solutions.[6]

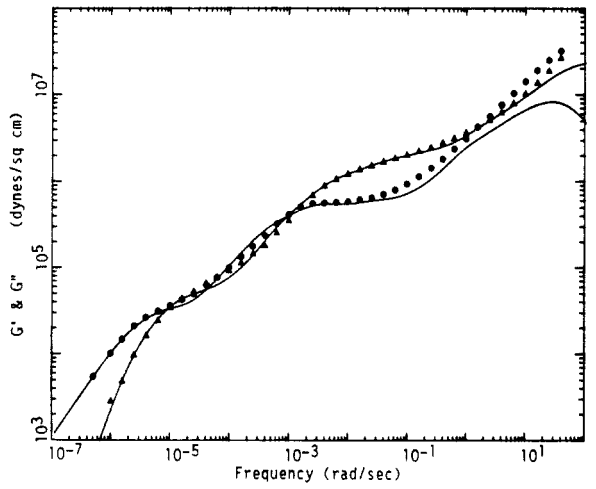


**Figure 10.** Same as Figure 1 for the F80/F10 = 25/75 blend.

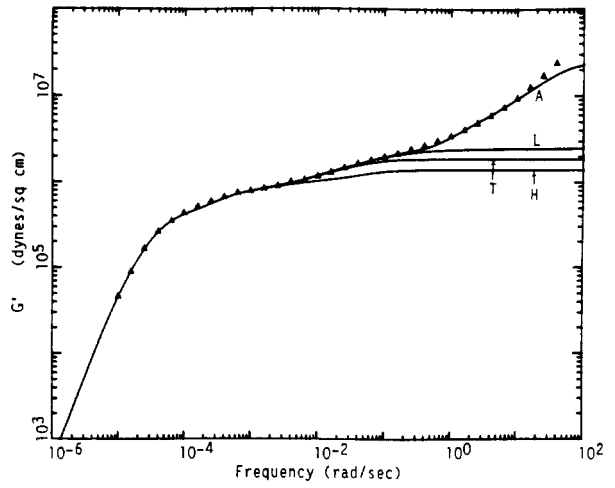


**Figure 11.** Comparison of the measured (▲) and calculated (—) spectra of the storage modulus $G'$ for the F35/F4 = 75/25 blend. Also shown are the separate contributions of the $\mu_A(t/\tau_A)$ process (A); the intrinsic relaxation (containing the $\mu_X(t)$, $\mu_B(t)$, and $\mu_C(t)$ processes) of the low MW component (L); the $\mu_T(t/\tau_T)$ process (T); and the intrinsic relaxation of the high MW component (H). See the text for details.

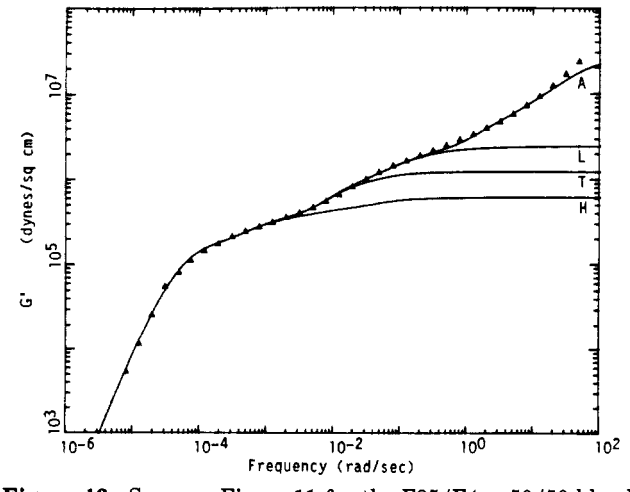


**Figure 12.** Same as Figure 11 for the F35/F4 = 50/50 blend.

For illustrating the contributions of the various processes to the total linear viscoelastic relaxation, it is luminous to show the separate calculated $G'(\omega)$ curves corresponding respectively to including all processes, excluding the $\mu_A(t)$ process, excluding both the $\mu_A(t)$ process and the intrinsic relxation of the low MW component, and finally excluding the regional constraint release process $\mu_T(t)$ as well. The

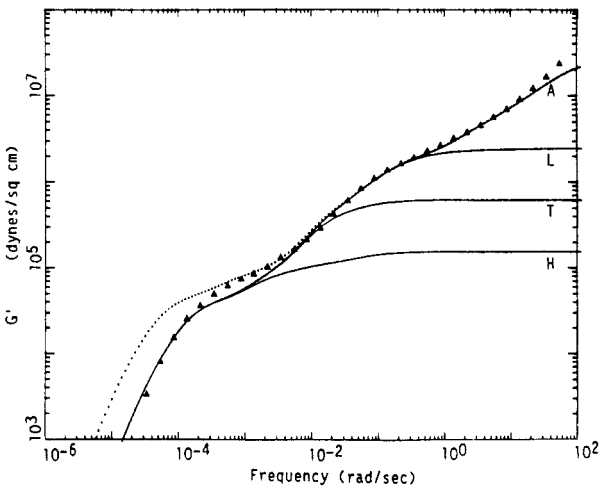


**Figure 13.** Same as Figure 11 for the F35/F4 = 25/75 blend. Also shown is the curve (···) calculated with $M_e''/M_e = 1.5$ for comparison with the solid line calculated with $M_e''/M_e = 3$.

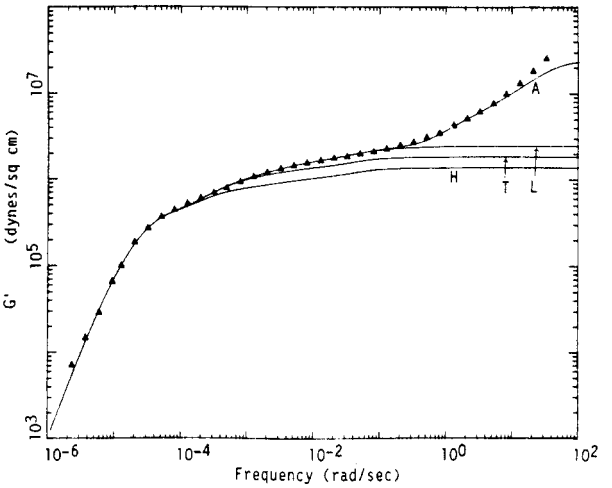


**Figure 14.** Same as Figure 11 for the F35/F10 = 75/25 blend.

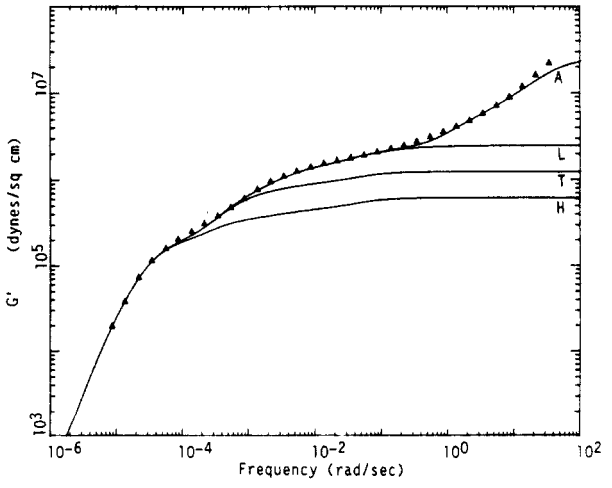


**Figure 15.** Same as Figure 11 for the F35/F10 = 50/50 blend.

calculated curves together with the experimental data are shown in Figures 11–20, corresponding to Figures 1–10, respectively.

In each figure (Figures 11–20), the lowest curve (denoted as H) indicates the contribution from the high MW component only, which has a plateau modulus of $G_N W_H^2$. The region (referred to as the T region below) between the lowest two curves (T and H) is the contribution from the $\mu_T(t)$ process, arising from the coupling between the high and low MW components; the region (referred to as the

**Table I**
**$M_n/M_e$ Values of the Listed Binary Blends and the Values of the Parameters $K'/K$, $K_L$, $K_L/K_H$, $M_e''/M_e$, and $S$ Used in Calculating Their Linear Viscoelastic Spectra[a]**

| samples | $M_n/M_e$ | $G_N/G°_N$ | $K'/K$ | $10^8K_L$ | $K_L/K_H$ | $M_e''/M_e$ | $S$ |
|---|---|---|---|---|---|---|---|
| F35/F4 = 75/25 | 9.49 | 0.98 | 2.8 | 1.42 | 1.25 | 1.19 | 7 |
| F35/F4 = 50/50 | 5.78 | 0.95 | 2.3 | 1.26 | 1.25 | 1.7 | 7 |
| F35/F4 = 25/75 | 4.16 | 0.95 | 1.8 | 1.37 | 1.25 | 3.0 | 7 |
| F35/F10 = 75/25 | 16.1 | 1 | 3.2 | 1.3 | 1.15 | 1. | 7 |
| F35/F10 = 50/50 | 11.6 | 1 | 2.8 | 1.2 | 1.15 | 1.14 | 7 |
| F35/F10 = 25/75 | 9.03 | 1 | 2.7 | 1.18 | 1.15 | 1.5 | 7 |
| F80/F4 = 50/50 | 6.29 | 1 | 2.6 | 1.25 | 1.3 | 1.75 | 7 |
| F80/F4 = 25/75 | 4.35 | 1 | 2.2 | 1.4 | 1.3 | 3.4 | 7 |
| F80/F10 = 50/50 | 13.1 | 1 | 3.8 | 1.3 | 1.3 | 1.5 | 7 |
| F80/F10 = 25/75 | 9.47 | 1 | 3 | 1.25 | 1.3 | 2.4 | 7 |
| F10 | | | | 1.2 | | | |
| | | | | av 1.29 ± 7% | | | |

[a] Shown in Figures 1–22. $G°_N$ is the plateau modulus of the monodisperse melt used in calculating the spectra; $G_N/G°_N$ is the shifting factor along the modulus coordinate in superposing the measured spectra of the binary blends onto the calculated as shown.

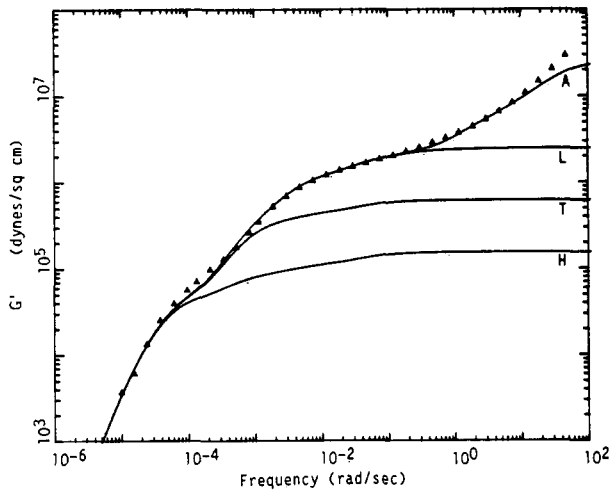


**Figure 16.** Same as Figure 11 for the F35/F10 = 25/75 blend.

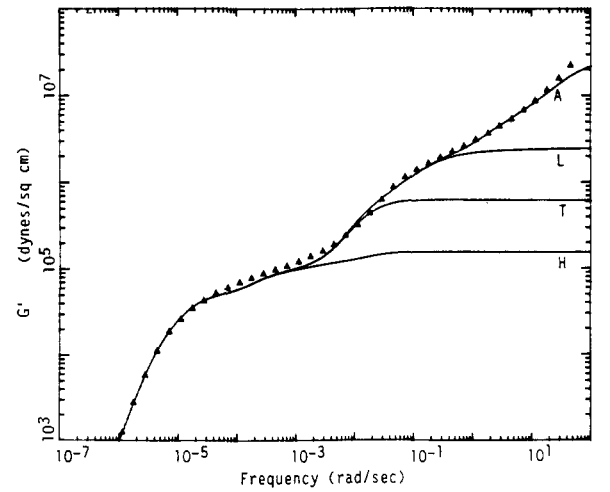


**Figure 18.** Same as Figure 11 for the F80/F4 = 25/75 blend.

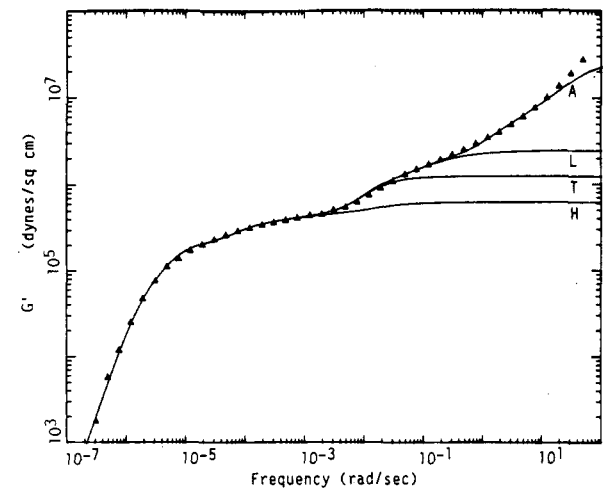


**Figure 17.** Same as Figure 11 for the F80/F4 = 50/50 blend.

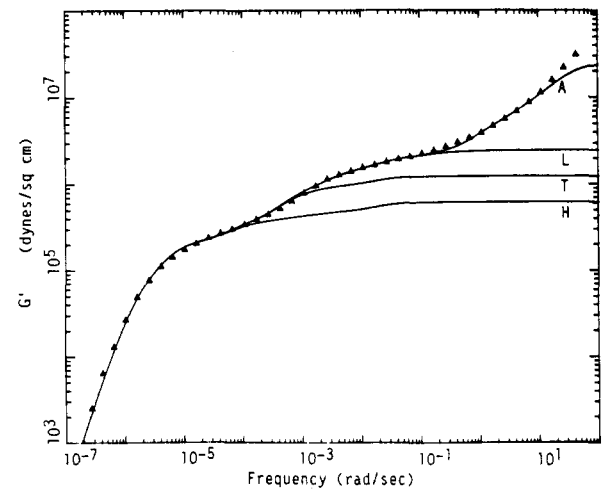


**Figure 19.** Same as Figure 11 for the F80/F10 = 50/50 blend.

L region below) between curve L and curve T is the contribution from the intrinsic relaxation (including the $\mu_X(t)$, $\mu_B(t)$, and $\mu_C(t)$ processes) of the low MW component; and the region (referred to as the A region) between curve A and curve L is contributed from the $\mu_A(t)$ process, which is shared by both the high and low MW components (see eq 1).

In the A and L regions, the theoretical $G'(\omega)$ curve is virtually only affected by the $K_L$ values and the $K'/K$ (or more appropriately $K'/K_L$: the obtained $K$ values differ from those of $K_L$ by less than 15%) ratios. In Figure 5, we also show the theoretical $G'(\omega)$ and $G''(\omega)$ curves (the dotted lines) calculated with $K'/K$ = 3.36 for comparison with the solid lines calculated with $K'/K$ = 2.8. The differences between the two sets of theoretical curves show the sensitivity of the calculated line shapes to the variation of the $K'/K$ value. The $G'(\omega)$ curve (which instead of $G''(\omega)$, should be the one to be considered for determining agreement between theory and experiment) of $K'/K$ = 2.8 clearly has a better agreement with the experimental results. We have concluded that the tube renewal process is negligible in a nearly monodisperse sample. Then the $K_L$ constant in the L region should be independent of the MW of the high MW component (F80 or F35) and its weight fraction ($W_H$). This is clearly indicated in eq 1. All the theoretical curves shown in Figures 1–20 are calculated

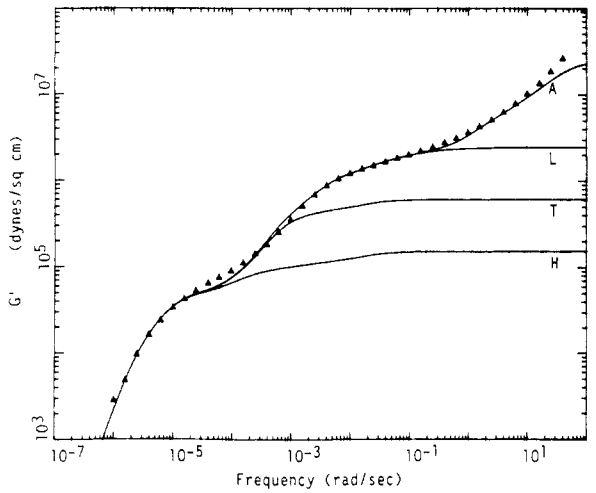


**Figure 20.** Same as Figure 11 for the F80/F10 = 25/75 blend.

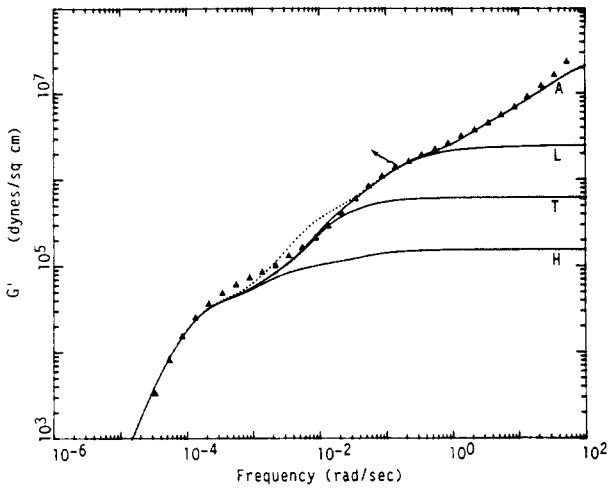


**Figure 21.** Same as Figure 11 for the F35/F4 = 25/75 blend. Also shown is the curve (···) calculated with $S = 16$ for comparison with the solid line calculated with $S = 7$. See the text for the details.

by using $K_L = 1 \times 10^8$. From the shifting factors between the measured and calculated curves, we have obtained the $K_L$ values for the different sample as listed in Table I.

In matching the measured data points to the theoretical curves in the L region, the modulus values of the different samples are the same within very small experimental error. This is indicated by the $G_N/G_N^\circ$ values listed in Table I. The constancy of the $G_N$ values is a very important factor in obtaining the reliable $K_L$ values. The obtained $K_L$ values are, indeed, very constant with a standard deviation of only 7%. Examining the closeness of agreement between the calculated curves and the experimental points, small additional errors (5–10%) are possible. In any case, the results are in very good agreement with what we have expected.

In the T region, the theoretical curve is mainly affected by the $S$ value. $S = 7$ describes very well all the spectra (Figures 1–20). In Figure 2, we have also shown the theoretical curves (the dotted lines) of $G'(\omega)$ and $G''(\omega)$ calculated with $S = 10$. The differences between the two sets of theoretical curves of $S = 7$ and $S = 10$ are quite noticeable. The comparison shows the sensitivity of the calculated line shapes in the T region (also see Figure 12) to the variation of the $S$ value. By examination of the differences between the calculated and measured spectra as detailed in Figures 1–20, it can be concluded that all the spectra are described in *a very consistent way* by the constant $S = 7$ with a possible uncertainty of less than 20%. We have more to say about the constancy of the $S$ value below.

In the terminal region associated with the high MW component (the terminal corner of the H curve), the spectra are sensitive to both $K_L/K_H$ and $M_e''/M_e$. The $M_e''/M_e$ values of the samples F35/Y = 75/25, 50/50, and F80/Y = 50/50 are predetermined from the shifting factors ($\tau_C''/\tau_C$) as described above. The obtained best values for the $K_L/K_H$ ratios (see Table I) are very reasonable according to what we have learned in the line-shape analyses for nearly monodisperse melts and concentrated solutions: namely, $K_H$ is slightly (20–30%) smaller than $K_L$ because of the broader MWD and low MW tail in the high MW component (see ref 3 for detailed explanation). The obtained $K_L/K_H$ values are then used to obtain the best $M_e''$ values for the samples: F35/Y = 25/75 and F80/Y = 25/75 from the line-shape analyses.

To illustrate the variation of the spectrum line shape with the change in $M_e''/M_e$ values, as an example, we show a series of theoretical curves calculated with $M_e''/M_e = 1$, 1.5, 2, 2.5, and 3 for F35/F10 = 25/75 in Figure 6. The curve $M_e''/M_e = 1.5$ is in best agreement with the experimental results. The line shape in the A and L regions is virtually not affected by the variation of the $M_e''/M_e$ ratio. Thus, the $K_L$ values and the $K'/K$ (or equivalently $K'/K_L$) ratios (listed in Table I), which we have obtained from matching the calculated and measured line shape in the A and L region, are independent of any possible uncertainties of the $M_e''/M_e$ ratios.

Between the tail of the T region and the terminal corner of the H region, the experimental values of F35/F4, F35/F10, F80/F4, and F80/F10 = 25/75 (Figures 3, 6, 8, and 10, respectively) are all noticeably higher than the theoretical values. This is so most likely because the tube size enlargement effect in this region is not as large as that in the last relaxation region (after the terminal corner). In Figure 13, we show the theoretical curves calculated with both $M_e''/M_e = 1.5$ (the dotted line) and $M_e''/M_e = 3$ (the solid line). The experimental data points appear to transit from the line of $M_e''/M_e = 1.5$ to the line of $M_e''/M_e = 3$. Note that in the high-frequency region, the spectrum is virtually unaffected by the variation of the $M_e''/M_e$ ratio.

The experimental values, being larger than the theoretical values calculated from $M_e''/M_e = 3$ in the above mentioned region, cannot be accounted for by increasing the $S$ value. In Figure 21, we show the theoretical curve of $G'(\omega)$ for F35/F4 = 25/75 calculated with $S = 16$ and $M_e''/M_e = 3$ (the dotted line), together with the solid line calculated with $S = 7$ and $M_e''/M_e = 3$. Clearly, increasing the $S$ value from 7 to 16 causes an increase of the theoretical values in a wrong region.

In a Rouse tube model,[9-11] the characteristic relaxation time $\tau_T$ is proportional to $W_H^{-2}$. In other words, $\tau_T$ for F35/F4 = 25/75 should be four times longer than that for F35/F4 = 50/50. We have already shown that $S = 7$ described very well all the spectrum line shapes (Figure 1–20) in a consistent way. Here, let's allow that $S = 7$ is the best for F35/F4 = 50/50. Then one would expect $S = 28$ for F35/F4 = 25/75 according to the "Rouse tube" model. Figure 21 clearly shows that this would not be the case (also see the Appendix).

In Figure 22, as an example, we show the A, L, T, and H contributions to the total $G''(\omega)$ spectrum curve of F80/F10 = 50/50. The calculated curves in Figure 22 as well as in the figures showing the linear viscoelastic spectra of the samples containing F80 are somewhat wavy in the terminal region. The wavy nature of the curves is caused by the discrete three-(sub)component MWD used in the

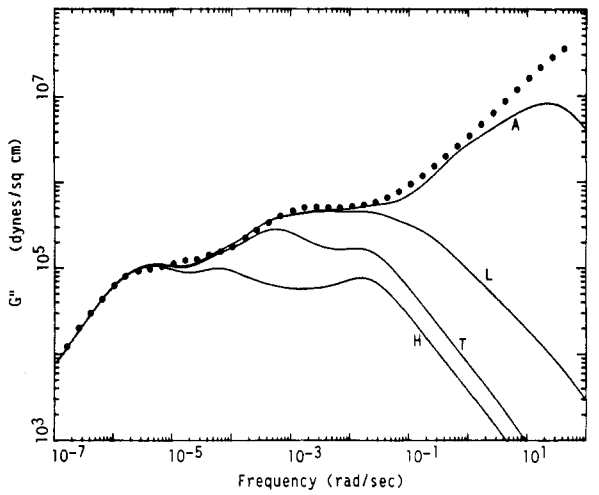


**Figure 22.** Comparison the the measured (●) and calculated (—) spectra of the loss modulus $G''$ for the F80/F10 = 50/50 blend. Also shown are the separate contributions of the $\mu_A(t/\tau_A)$ process (A); the intrinsic relaxation of the low MW component (L); the $\mu_T(t/\tau_T)$ process (T); and intrinsic relaxation of the high MW component (H).

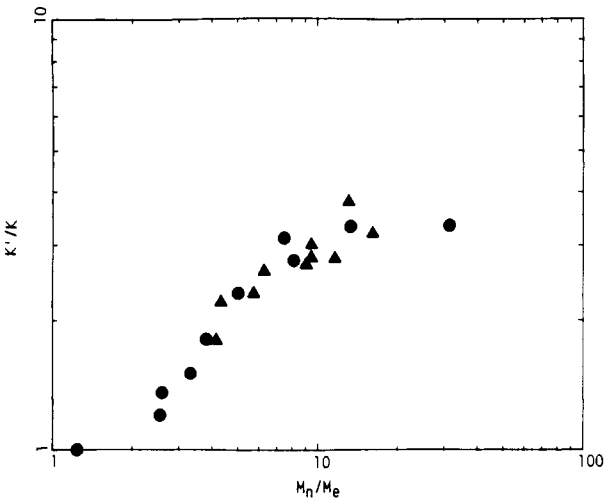


**Figure 23.** $K'/K$ values are a function of normalized number-average MW ($M_n/M_e$), including data for the nearly monodisperse melts (●) and the binary blends (▲).

calculation. The line shapes associated with the samples containing F35 are less wavy, because the three (sub)-components in F35 are not as far apart as in F80.

## V. The $K$ Constants

As described in section IV the $K_L$ values of all the studied binary blend samples are very constant. We have measured the samples of F35/F10 = 50/50 and pure F10 at the same termperature sequentially. The $K_L$ values (or $K$ for the pure F10) obtained are virtually identical, as listed in Table I. These are very important results. The diffusion data[13] indicate that the tube renewal process is negligible for MW above 100 000 and observable below 100 000 in the case of monodisperse polystyrene samples. However, analyzing the viscoelastic spectrum line shapes in terms of the proposed monodisperse theory, we have shown and concluded that the tube renewal process is negligible to a MW as low as $1.24M_e$ as long as the MWD is very narrow.[2-4] We have explained the difference between the diffusion and viscoelasticity results as due to the chain length fluctuation process being effective in the case of viscoelastic relaxation but not in the case of diffusion motion.[5] We have shown that the pure reptation times calculated from the viscoelastic data in terms of the monodisperse theory (corrected for the chain length fluctuation effect) are in quantitative agreement with those calculated from the diffusion data. The present results of $K_L$ being constant confirm the previous conclusion.

As described in paper 1,[1] we have observed that in a X/Y blend, there is a MW region of Y smaller than the MW of X, in which the $\tau_C''/\tau_C$ ratio (for the X component) is 1 and is independent of the MW of Y. The present result that $K_L$ is constant extends the MW region of Y beyond the MW of X. Furthermore, for MW of Y > MW of X in a X/Y blend, the constraint release process, $\mu_T(t/\tau_T)$, cannot occur on X (which would be caused by the reptation of Y), as indicated by eq 1 and supported by the line-shape analyses described in section IV.

Then we can summarize the transitions as follows. Begin at MW of Y << MW of X in a $X/Y$ blend at a certain weight fraction ratio of X and Y (under the condition that the high MW component is always in the concentrated regime). First, the $\tau_C''/\tau_C$ ratio (for X) is less than one and dependent on the MW of Y. As the MW of Y increases, the system will enter a region where $\tau_C''/\tau_C = 1$ (for X) and is independent of the MW of Y. In these first two regions, the $\mu_T(t/\tau_T)$ process on the X chain tube caused by the reptation motion of the Y chains occurs. As the MW of Y approaches that of X, $\mu_T(t/\tau_T)$ becomes 1 and independent of time (i.e., the tube renewal process disappears). At MW of Y ~ X, the monodisperse theory and the linear additivity law are applicable. When the MW of Y becomes larger than that of X, the $\mu_T(t/\tau_T)$ process on the X chain tube, as when (nearly) monodisperse, does not occur (i.e., $\mu_T(t/\tau_T) = 1$). Eventually, X and Y exchange their roles in affecting each other.

Another important and interesting aspect of the $K$ constants is the MW dependence of the $K'/K$ ratio. In monodisperse melt systems, $K'/K$ has a plateau value of about 3.3 (after about 30% correction for the MWD effect) in the high normalized MW region.[3] At $M/M_e \sim 10$, the $K'/K$ ratio starts to decrease with decreasing MW and reaches a limiting value of 1 at $M/M_e \sim 1$.

It has been proposed[2-4,6] that for $K'/K > 1$, the friction coefficient for the polymer chain segment to move in the direction perpendicular to the chain contour is larger than that along the chain contour. This is a reasonable explanation, if we consider that a certain local extra free volume is associated with the polymer chain end. This extra free volume is always available to the $\mu_X(t)$, $\mu_B(t)$, and $\mu_C(t)$ processes, in which the polymer chain moves along the chain contour. On the other hand, the portion of this extra free volume available to the $\mu_A(t)$ process of a polymer chain depends on the concentration of free chain ends of polymer molecules surrounding it. Thus, the $K'$ value extracted from the $\mu_A(t)$ process is MW dependent. Furthermore, the $K'/K$ value approaching the value 1 at $M/M_e \sim 1$ supports this explanation.[3]

In a binary blend (in the a and b regions of paper 1), the $\mu_A(t)$ process is shared by both the low MW and high MW chains as indicated by eq 1. Very interestingly and significantly, we have found that the MW dependence of the $K'/K$ ratio (see the values listed in Table I) falls on the universal curve of $K'/K$ vs $M/M_e$ of the monodisperse systems very well if a normalized number-average MW, $M_n/M_e$, is used. This is shown in Figure 23. If normalized weight-average MW, $M_w/M_e$, were used to plot the $K'/K$ data of the binary blend samples, the correlation would be totally lost. This result clearly indicates that $M_n$ is the one that is involved in the phenomenon. That $M_n$ is involved strongly supports the explanation that we have proposed for $K'/K > 1$ and $K'$ being MW dependent, be-

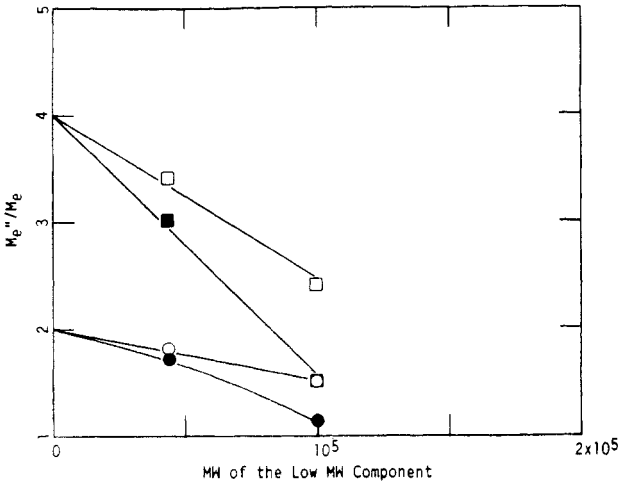


**Figure 24.** $M_e''/M_e$ values as a function of the MW of the low MW component in the four series of binary blends: F35/Y = 50/50 (●), F35/Y = 25/75 (■), F80/Y = 50/50 (○), and F80/Y = 25/75 (□).

cause $M_n$ rather than $M_w$ is directly related to the concentration of polymer chain ends. In nearly monodisperse melt systems, we do not need to make the distinction between $M_w$ and $M_n$. For the accuracy involved here, they are practically the same.

It is interesting to compare the MW dependence of the $K'/K$ ratio in monodisperse melts and binary blends to that in concentrated solutions (the c region; see paper 1). In the c region, the MW of the high MW component ($M_H$) has to be normalized with respect to $M_e'$ ($=M_eW_H^{-1}$) so that the $M_H/M_e'$ dependence of $K'/K$ falls on the same universal curve.[6] The MW of the low MW component in the c region is smaller than $M_e$. In this case, using number-average MW (calculated by including both the high and low MW components) is not the proper way to show the MW dependence of $K'/K$. As pointed out previously,[2-4,6] the anisotropic free volume distribution in the polymer medium, which causes $K'/K > 1$, has much to do with chain entanglement. In the c region, the chain entanglement MW is $M_e'$, which affects the microscopic free volume anisotropic distribution.[6] The two ways of showing the MW dependence of $K'/K$ (namely, $K'/K$ vs $M_n/M_e$ in the a region and $K'/K$ vs $M_H/M_e'$ in the c region) strongly suggest a transition region in the b region, which could be very complex. This may be closely related to merge of the $\mu_T(t/\tau_T)$ process into the $\mu_A(t/\tau_A)$ process in passing through the b region (see the Appendix of ref 6). $\mu_A(t/\tau_A)$ is described by the Rouse process (see eq 4 and 5 of paper 1), but not $\mu_T(t/\tau_T)$ (see the Appendix).

## VI. Tube Size Enlargement

As listed in Table I, the $M_e''$ values of the samples F35/Y = 75/25, 50/50 and F80/Y = 50/50 are calculated from the obtained shifting factors $\tau_C''/\tau_C$ according to eq 3. From the line-shape analyses of these samples, very reasonable $K_L/K_H$ values are obtained, which are then used to determined the $M_e''$ values of the other samples: F35/Y = 25/75 and F80/Y = 25/75.

In Figure 24, we show the $M_L$ dependence of the $M_e''$ values of the four sets of samples: F35/Y = 50/50, 25/75 and F80/Y = 50/50, 25/75. As explained in paper 1, the extrapolations of $M_e''$ vs $M_L$ to $M_L = 0$ should give the $M_e'$ values in the concentrated solutions as given by

$$M_e' = M_eW_H^{-1} \quad (4)$$

The results shown in Figure 24 clearly indicate that the $M_e'$ values calculated from eq 4 and obtained from the extrapolations are in good agreement.

## VII. Conclusion

Two series of binary blend samples (F80/Y and F35/Y) have been measured for their linear viscoelastic spectra. The line shapes of the spectra are uniquely described by the proposed $G(t)$ functional form in a consistent manner. The obtained $K_L/K_H$ values (<1.3) are very reasonable. Furthermore, the obtained $K_L$ values are independent of MWs and weight fractions of the high and low MW components and are in close agreement with that of a pure melt (F10). This in one of the most direct ways confirms the conclusion that the tube renewal process is negligible in a (nearly) monodisperse system, which has been drawn from an extensive line-shape analysis of the linear viscoelastic spectra of nearly monodisperse samples.[2-8]

The $M_e'$ values obtained from the extrapolation of $M_e''$ vs $M_L$ to $M_L = 0$ are in good agreement with the theoretical values. This strongly supports the validity of the phenomenological description of the tube enlargement effect by using an effective entanglement MW value: $M_e''$. Such a phenomenological description is built upon the fundamental understanding of the polymer dynamics in the monodisperse melts and concentrated solutions in terms of the proposed general linear viscoelastic theory.[2-7] The present successful line-shape analyses, on the one hand, show the different dynamic modes involved in a binary blend and, on the other hand, are an extension of the consistency of the monodisperse theory in explaining the linear viscoelastic behavior quantitatively. The constraint release process, while negligible in a monodisperse system, occurs in a binary blend. It is shown that the regional constraint release process is closely related to the reptation motion of the low MW component. The proportional constant $S$ between the regional constraint release characteristic time $\tau_T$ and the reptation time $\tau_C^L$ of the low MW component is a constant and is independent of MWs and weight fractions of the high and low MW components of the studied binary blend samples. This is a very significant result. This means that the regional constraint release process should not be described by the "Rouse tube" type of motion in the $W_H$ range of the studied samples. $S$ being constant implies that the regional constraint release process is very local; namely, motion at one point of the chain tube is not correlated with that at another point in the same region. A theoretical calculation of the $S$ parameter or its equivalent will shed light on the dynamic behavior of the regional constraint release process.

## Appendix: The Choice of a Phenomenological Functional Form for $\mu_T(t/\tau_T)$

When the regional constraint release process as included in eq 1 was first recognized in 1983, I also found that a box-type relaxation functional form for $\mu_T(t/\tau_T)$ similar to eq 2 worked best.[12] The present study involving more careful experimental measurements and data analyses confirms the earlier findings. During these few years, research in the field of binary blend systems have been very active. The following discussions of eq 2 and its role in eq 1 with respect to some of the published results by others may be enlightening and complementary to the main test, whose main objective is to document the work.

In more traditional ways of data analyses, Masuda et al.[14] and Watanabe and Kotaka[15] have studied the binary blend systems. The blending laws that they have proposed have bases similar to that contained in eq 1. Comparing the blending law (eq 1 of ref 14) proposed by Masuda et al. with eq 1 (or eq 2 of paper 1), we see that one of the terms, $H_{12}(\tau/\lambda_{12})$ (1 is equivalent to L and 2 equivalent to

H), of Masuda is basically equivalent to $\mu_T(t/\tau_T)[B^H\mu_B(t/\tau_B^H) + C^H\mu_C(t/\tau_C^H)]$. In other words, $H_{12}(\tau/\lambda_{12})$ contains the intrinsic relaxation processes associated with the high MW component. $\tau_{12}$ obtained by Masuda et al. increases as $W_H$ (or $W_2$) increases, in contradiction to that expected from a Rouse process. It appears that the $W_H$ dependence of $\tau_{12}$ of Masuda can qualitatively be explained by the tube size enlargement effect, which becomes more enhanced and reduces $\tau_C^H$ further with decreasing $W_H$. Similar to the functional form of $\mu_T(t)$ given by eq 2 and $[B\mu_B(t) + C\mu_C(t)]$ (both are box-type functions, and the product of two box type functions is a box type), the shape of $H_{12}(\tau)$ they have obtained looks like a box type.

A similar comparison of the blending law proposed by Watanabe and Kotaka (eq 12 of ref 15) with that of Masuda et al. and eq 1 can be made. Basically because they subtracted a contribution of $W_2H_2^b(\tau)$ in the short-time region ($\tau < \tau_{11}$; $\tau_{11} \sim \tau_C^L$), their obtained $H_{12}^w(\tau)$ unlike $H_{12}(\tau)$ of Masuda et al. is a wedge type.

In summary, $\mu_T(t)$ is best described by a box-type relaxation function similar to eq 2. A Rouse tube model, as shown by Pearson,[11] leads to a wedge-type function. In addition to $\tau_T$ being independent of $W_H$ explained in the test, this is another reason why $\mu_T(t)$ should not be described by a Rouse tube model.

**Registry No.** Polystyrene, 9003-53-6.

## References and Notes


(1) Lin, Y.-H. *Macromolecules*, preceding paper in this issue.
(2) Lin, Y.-H. *Macromolecules* **1984**, *17*, 2846.
(3) Lin, Y.-H. *Macromolecules* **1986**, *19*, 159.
(4) Lin, Y.-H. *Macromolecules* **1986**, *19*, 168.
(5) Lin, Y.-H. *Macromolecules* **1985**, *18*, 2779.
(6) Lin, Y.-H. *Macromolecules* **1987**, *20*, 885.
(7) Lin Y.-H. *Non-Newtonian Fluid Mech.* **1987**, *23*, 163.
(8) Lin, Y.-H. *Macromolecules* **1987**, *20*, 3080.
(9) Struglinski, M. J.; Graessley, W. W. *Macromolecules* **1985**, *18*, 2630.
(10) Doi, M.; Graessley, W. W.; Helfand, E.; Pearson, D. S. *Macromolecules* **1987**, *20*, 1900.
(11) Pearson, D. S. *Rubber Chem. Technol.* **1987**, *60*, 439.
(12) Lin, Y.-H. Unpublished results. Also see ref 52 of ref 9.
(13) Green, P. F.; Mills, P. J.; Palmstrom, C. J.; Mayer, J. W.; Kramer, E. J. *Phys. Rev. Lett.* **1984**, *53*, 2146.
(14) Masuda, T.; Yoshimatsu, S.; Takahashi, M.; Onogi, S. *Polym. Prepr. Jpn.* **1983**, *32*(9), 2365.
(15) Watanabe, H.; Kotaka, T. *Macromolecules* **1984**, *17*, 2316.


# Short-Range Fluctuations in the Spinodal Decomposition of Binary Polymer Mixtures


**P. Cifra,[†] F. E. Karasz,*[‡] and W. J. MacKnight[‡]**

*Polymer Institute, Slovak Academy of Science, 842 36 Bratislava, Czechoslovakia, and Department of Polymer Science and Engineering, University of Massachusetts, Amherst, Massachusetts 01003.*

*Received November 29, 1988*


ABSTRACT: Isothermal demixing after an instantaneous quench to below the spinodal of a binary polymer mixture was studied by using computer-simulation methods. Short-range fluctuations, corresponding to a large wavenumber $q$, were followed during the demixing. The results obtained provide a useful supplement to those based on a linearized version of Cahn's theory of spinodal decomposition (SD). The latter theory applies to *small* $q$ regimes and to scattering experiments that cover a range of fluctuation wavelengths typically larger than the size of the polymer coils. However, fluctuations in wavelength on the order of the interaction range, i.e., the nearest-neighbor distance in the mixture, are not adequately described by the linearized theory; deviations are observed at very early stages of phase decomposition. In this regime thermodynamic, rather than diffusional, factors are paramount. In the present study spinodal decomposition for mixtures on a three-dimensional cubic lattice were simulated, and the corresponding kinetics were evaluated for a range of quench depths.


## Introduction

The subject of polymer blends is now one of the most widely studied areas in the field of polymer material science. A thorough knowledge of the thermodynamics of polymer mixtures is necessary in the preparation and processing and in the control of the morphology of polymer blends. One special area of interest in the study of the thermodynamics of polymer mixtures is phase separation proceeding by spinodal decomposition (SC). In this process, a quench to an unstable region of the phase diagram is followed by a rapid appearance of a characteristic dimension, $2\pi/q$, throughout the system, where the parameter $q$ is the wavelength of a sinusoidally modulated two-phase domain. The two-phase structure that appears is uniform and highly interconnected with a characteristic mesh size of concentration fluctuations. This process therefore differs from the nucleation process, which starts nonuniformly at discrete isolated points.

Spinodal decomposition was first observed in mixtures of low molecular mass components,[1] and interest in this field was later extended to polymer mixtures.[2] Such mixtures are particularly well suited for these studies because of their high viscosity; thus the nucleation and growth mechanism that is characteristic for quenches to the metastable regime does not occur during the rapid quench from a stable through the metastable to the unstable regime of the phase diagram. Nishi et al.[2] were the first to apply the linearized Cahn–Hilliard[1] theory of SD used for mixtures of low molecular mass constituents to phase separation in polymer blends. Many studies have since appeared using light-scattering,[3,4] X-ray,[5] and small-angle neutron-scattering techniques[6] for investigations of the concentration fluctuations in model systems. Scattering studies can investigate fluctuations in a $2\pi/q$ range that is larger than the typical size of a polymer coil, say, 100 Å. It is obvious that for fluctuations in this range the linearized SD theory developed for low molecular weight mixtures is applicable, and it has been found that


[†] Slovak Academy of Science.
[‡] University of Massachusetts.


0024-9297/89/2222-3089$01.50/0 